ISSN 1054-660X, Laser Physics, 2012, Vol. 22, No. 1, pp. 81–86.

Diode-Pumped Acousto-Optically Q-switched High-Repetition-Rate Nd:YAG Lasers at 946 and 473 nm by Intracavity Frequency-Doubling[1]

F. Chen[a, b, *], X. Yu[b], J. Guo[a], L. H. Guo[a], G. L. Yang[a], J. J. Xie[a], L. M. Zhang[a], Y. M. Geng[a], S. M. Li[a], D. J. Li[a], C. L. Shao[a], F. J. Meng[a], C. S. Zhang[a], and R. P. Yan[b]

[a] *State Key Laboratory of Laser Interaction with Matter, Changchun Institute of Optics, Fine Mechanics and Physics, Chinese Academy of Sciences, Changchun, 130033 China*

[b] *National Key Laboratory of Science and Technology on Tunable Laser, Harbin Institute of Technology, Harbin 150080 China*

*e-mail: feichen@yahoo.cn

Received July 16, 2011; in final form, July 20, 2011; published online October 24, 2011

Abstract—A diode-pumped acousto-optically (AO) Q-switched high-repetition-rate Nd:YAG lasers at 946 and 473 nm by intracavity frequency-doubling were reported in this paper. Using a compact V-type laser cavity, a maximum average output power of 4.5 W 946 nm laser was obtained at an operating repetition rate of 10 kHz, corresponding to an optical conversion efficiency of 10.5% and a slope efficiency of 15.6%. With a BiBO crystal as the intracavity frequency-doubler, 1.35 W 473 nm pulsed laser was achieved at 10 kHz. The peak power of the Q-switched blue pulse was up to 4.1 kW, with a pulse width of 33.1 ns. Then, the long-term power instability was less than 1%. Moreover, stable pulsed operation of 946 nm and 473 nm lasers can even reach 50 kHz.

DOI: 10.1134/S1054660X11230034

1. INTRODUCTION

Continuous-wave (CW) blue lasers have many important applications such as high-density optical data storage, biological and medical diagnostics, and color displays, while pulsed blue lasers are demanded in some special cases such as submarine laser imaging and communication. For improving the speed and depth in submarine applications, high-repetition-rate, high-peak-power blue lasers are needed specially. Since the first diode-pumped CW 946 nm Nd:YAG laser was introduced by Fan and Byer in 1987, much more attention was paid on the development of high power CW 473 nm blue laser by frequency doubling technology [1–10]. For generating a pulsed laser and raising the laser peak power, Q-switch is an effective method. In 2002, Wang reported on the 473 nm blue laser with a peak power of 37 W and a pulse width of 23 ns by intracavity frequency-doubling of a passively Q-switched 946 nm Nd:YAG laser [11]. In 2000, Lutz obtained the pulsed 473 nm laser by using extra-cavity frequency-doubling of an electro-optic Q-switched 946 nm Nd:YAG laser, with a single pulse energy of 9 mJ and a pulse width of 25 ns at a repetition rate of 2.5 Hz [12]. In 2007, Chen demonstrated the pulsed 473 nm laser using intracavity frequency-doubling of an AO Q-switched 946 nm Nd:YAG laser, and a maximum output power of 2.25 W blue laser was achieved at 23 kHz, giving a peak power of 610 W and a pulse width of 160 ns [13]. In 2008, our group had present the pulsed 457 and 456 nm blue lasers by using intracavity frequency-doubling of diode-pumped AO Q-switched Nd-doped vanadate lasers in a Z-type laser cavity. At 20 kHz, peak powers of 175/193 W were obtained for 457/456 nm lasers, respectively, with the pulse width of 150/200 ns [14, 15]. The former results revealed that a high-repetition-rate pulsed 473 nm blue laser can be obtained by frequency-doubling of a diode-pumped AO Q-switched 946 nm Nd:YAG laser. To enhance the conversion efficiency from fundamental laser to second-harmonic laser, the intracavity frequency-doubling was preferred because of the low power intensity of the fundamental laser. However, the peak power of pulsed 473 nm laser is difficult to improve at a high-repetition-rate operation. Firstly, the stimulated emission cross section at 946 nm laser is only 4×10^{-20} cm^2, which is an order of magnitude smaller than that of 1064 nm transition [16]. Secondly, the re-absorption loss of quasi-three-level system is serious for there is considerable thermal population at the lower laser level, and this population value is about 8% at room temperature [17, 18]. Thirdly, the severe thermal lens effects limit the increase of pump power in a diode-end-pumping configuration, especially for Q-switched 946 nm Nd:YAG laser operation [19, 20]. Therefore, the increase of the laser peak power is restricted by a relative lower gain and longer pulse width of the 946 nm fundamental laser.

In this paper, we reported a high-repetition-rate 946 nm Nd:YAG laser and pulsed 473 nm blue laser. Using a compact thermal-insensitive V-type laser cav-

[1] The article is published in the original.

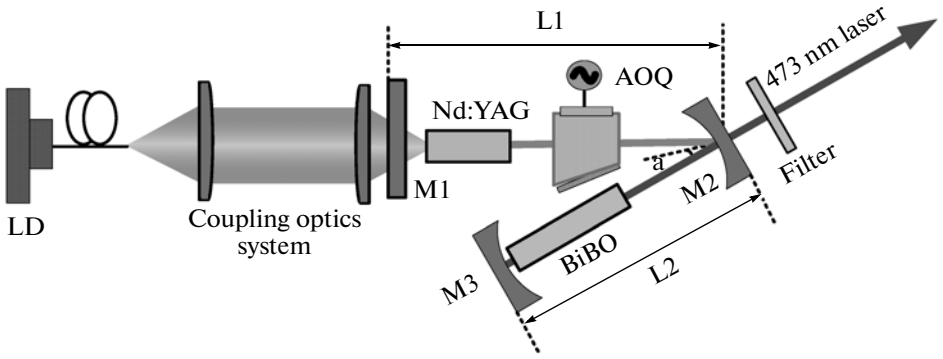

Fig. 1. Sketch of the experimental setup.

ity and a miniature AO Q-switch, an average output power of 4.5 W 946 nm laser was obtained at 10 kHz, with an optical conversion efficiency of 10.5% and a slope efficiency of 15.6%. With a BiBO crystal as intracavity frequency-doubler, a maximum average output power of 1.35 W 473 nm laser was achieved at 10 kHz, with a peak power of 4.1 kW and a pulse width of 33.1 ns. To the best of our knowledge, this is the highest peak power of 473 nm laser at high-repetition-rate operation by intracavity frequency-doubling.

2. EXPERIMENTAL SETUP

The experimental setup of the diode-pumped AO Q-switched Nd:YAG lasers at 946 and 473 nm by intracavity frequency-doubling is shown in Fig. 1. The pump source was a high brightness fiber-coupled laser-diode (HLU110F400, LIMO), which delivered a maximum output power of 110 W at 808 nm from the end of a fiber with 400 μm core in diameter and a NA of 0.22. The pump beam was coupled into the gain medium by a coupling optics system, which consisted of two identical plano-convex lenses with a coupling efficiency of 98%, and the pump beam spot radius generated in the crystal was ~200 μm. A conventional Nd:YAG crystal with a doping concentration of 0.5 at % and the dimensions of $3 \times 3 \times 4$ mm^3 was employed as a gain medium, for low doping concentration and short length crystals can minimize the re-absorption loss, up-conversion, concentration quenching and the amplified spontaneous emission (ASE) effect. The crystal wrapped with 0.05 mm thick indium foil was mounted in a copper micro-channel heat sink, and was cooled by water at the temperature of 10.0 ± 0.1°C. After good match between the pump wavelength and the absorption peak of the laser crystal was accomplished, ~60% pump power was absorbed by the laser medium. A 20 mm miniature AO Q-switch was employed in the laser cavity for generating short laser pulse. To prevent the more efficient four-level transitions at 1064 and 1342 nm, both sides of the crystal and the Q-switch were coated for high transmission (HT) at 946 nm ($T > 99.8\%$) and 808 nm ($T > 99\%$), while antireflection (AR) coatings at 1064 nm ($R < 1\%$) and 1342 nm ($R < 2\%$) were considered as well. The experiments were carried out with a compact V-type laser cavity, which was built by a flat dichroic input mirror M1, two concave mirrors M2 and M3. The curvature radius of M2 and M3 were 50 and 200 mm, respectively. In experiments, L1 and L2 were kept at 70 and 37 mm, respectively. The laser medium and the nonlinear crystal were placed near the M1 and M3, respectively. The folded angle (α) was set to be ~10°. Considering the thermal focal lens in the gain medium, the laser beam radius at the laser crystal (ω_L) and the nonlinear crystal (ω_N) were calculated by the software of Lascad (LAS-CAD GmbH), which are shown in Fig. 2. The beam radius in the BiBO crystal is ~49 μm, which would guarantee to achieve high efficient intracavity frequency-doubling. The cavity stability parameter (g_1g_2) shows that this laser cavity is thermal-insensitive, and it can be stably operated when the thermal focal length is not shorter than 40 mm.

3. EXPERIMENTAL RESULTS AND DISCUSSION

Removing the BiBO crystal from the laser cavity and replacing M3 by a plane output coupler mirrors with a transmissivity of 12.6% at 946 nm. Pulsed 946 nm laser characteristics were investigated firstly. Output laser spectra and power were measured by a fiber spectrometer (HR4000, Ocean Optics Inc.) and a laser power meter (PM30, Coherent Inc.), respectively. The Q-switched pulses were recorded by a digital oscilloscope (DPO 7104, Tektronix Inc.) and a fast photodiode (DET 210, Thorlabs Inc.) with a rising time of less than 1 ns. At 10 kHz, the dependence of average output power and pulse width for 946 nm laser on the incident pump power is shown in Fig. 3. It can be seen that, a maximum average output power of 4.5 W 946 nm laser was achieved at an incident pump power of 43 W, corresponding to an optical conversion efficiency of 10.5% and a slope efficiency of 15.6%. When the incident pump power was higher than 43 W,

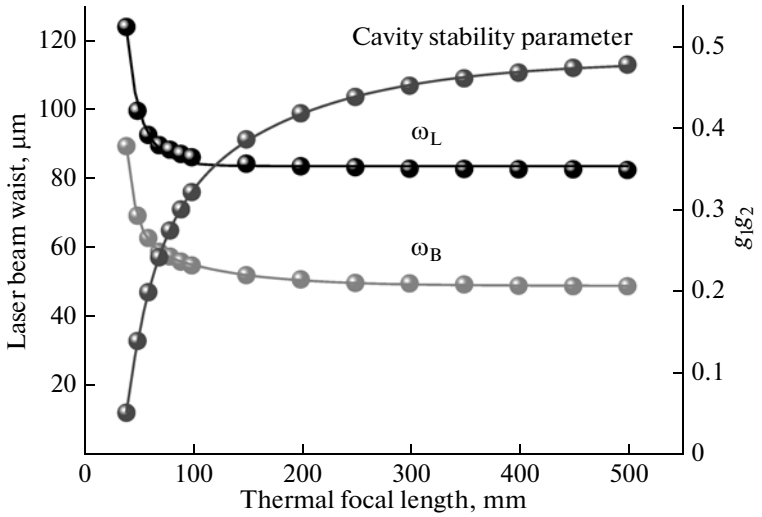

Fig. 2. Laser beam radius in Nd:YAG (ω_L) and BiBO (ω_B) crystals and the cavity stability parameter g_1g_2 versus the thermal focal length.

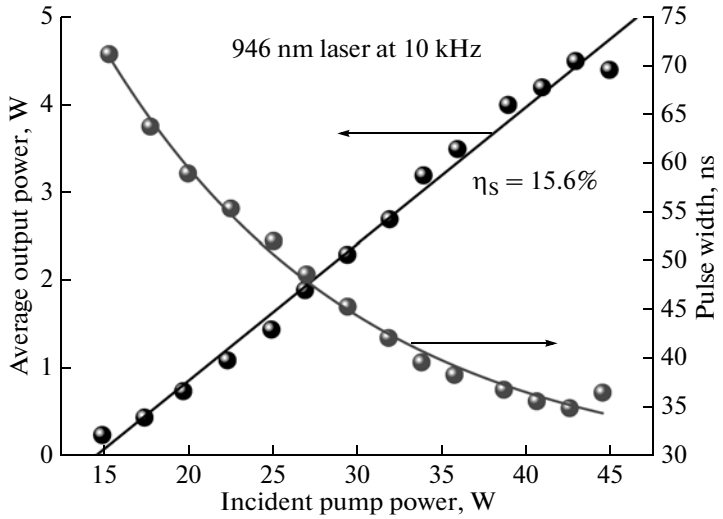

Fig. 3. Average output power and pulse width of 946 nm laser versus the incident pump power at the repetition rate of 10 kHz.

the output power would be reduced for the serious thermal lens effects. With the increase of the pump power, the pulse width was reduced. A minimum pulse width of 35 ns was achieved at the maximum output power. If the pump power was beyond 43 W, the pulse width would be increased, and it can be attributed to the transit time of the Q-switch was becoming longer for the depravation of the laser beam quality.

At the incident pump power of 43 W, the pulsed 946 nm laser performance from the repetition rate of 10 to 50 kHz was shown in Fig. 4. The pulse width was increased and the peak power was decreased evidently as the increase of the repetition rate. At 10 kHz, the highest peak power of 12.9 kW was obtained, with the minimum pulse width of 35 ns.

View of the advantages of large nonlinear coefficient and high laser damage threshold, a BiBO crystal with the dimensions of $3 \times 3 \times 15$ mm^3 was employed as the frequency doubler, which was placed near M3 in order to achieve high conversion efficiency from fundamental laser to second-harmonic laser. The crystal was cut for type I critical-phase-matching condition ($\theta = 159.5°$, $\varphi = 90°$) and installed in a copper holder whose temperature was precisely controlled by a thermal electric cooler with 0.1°C accuracy. Both facets of the nonlinear crystal were well polished and AR coated at 473 and 946 nm. Figure 5 shows the average output power and the pulse width of 473 nm laser as a function of the incident pump power at 10 kHz. With the increase of pump power, the output power was increased almost linearly and the pulse width would be

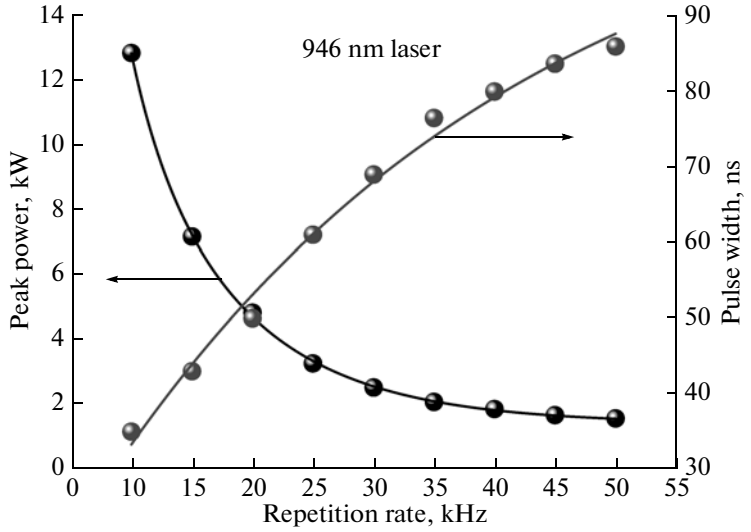

Fig. 4. Peak power and pulse width of 946 nm laser versus the operating repetition rate.

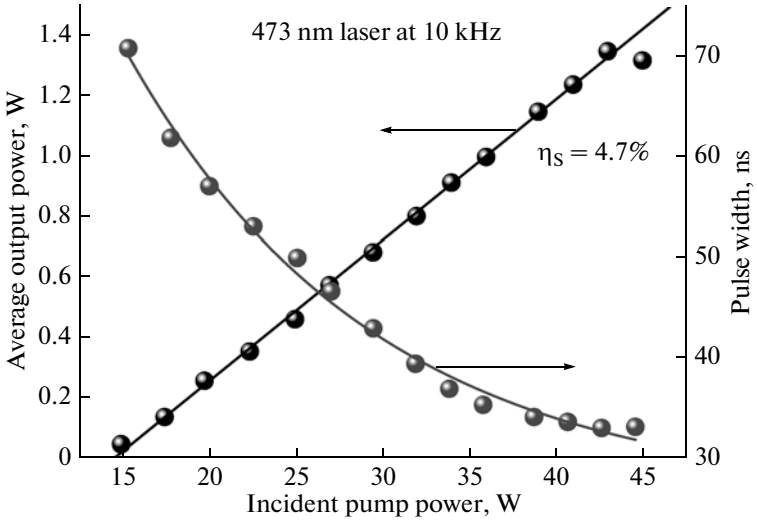

Fig. 5. Average output power and pulse width of 473 nm laser versus the incident pump power.

reduced. As a result, the maximum average output power of 1.35 W 473 nm laser was obtained at the pump power of 43 W, with an optical conversion efficiency of 3.1% and a slope efficiency of 4.7%, and the pulse width was 33.1 ns then.

At the pump power of 43 W, the pulsed 473 nm laser performance from the repetition rate of 10 to 50 kHz was also investigated, as present in Fig. 6. As it happened in the 946 nm fundamental laser, with the increase of the repetition rate, the pulse width was increased and the peak power was decreased for the blue laser. At 10 kHz, the highest peak power of 4.2 kW and the minimum pulse width of 33.1 ns were obtained. The pulse width was increased to 84.5 ns and the peak power was reduced to 0.49 kW at 50 kHz. At 60 kHz, there would be a slight reduction of the average output power for blue laser, but the pulse amplitudes jittered drastically, which indicated the laser gain at 946 nm was not enough to achieve a stable Q-switched operation beyond 50 kHz. The pulse trains and the typical pulse shapes of 473 nm blue laser at 10 and 50 kHz are shown in Figs. 7a and 7b, respectively. It can be seen that the peak to peak instability of pulse amplitude was increased markedly from 10 to 50 kHz.

The long-term power instability of the 473 nm blue laser was also studied. The time trace of the maximum average output power at 10 kHz is shown in Fig. 8. In 20 min, the fluctuation of the output power was less than 1%. No obviously so-called "blue problem" [21] in the intracavity frequency-doubling lasers was observed, which may be attributed to the precise tem-

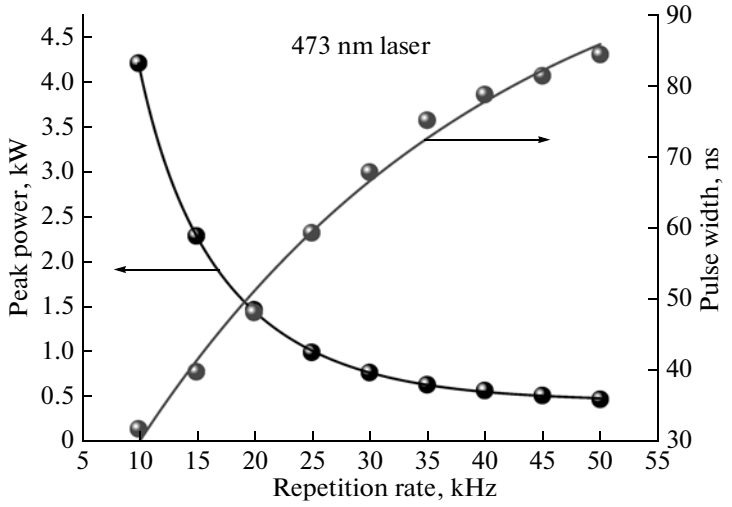

Fig. 6. Peak power and pulse width of 473 nm laser versus the operating repetition rate.

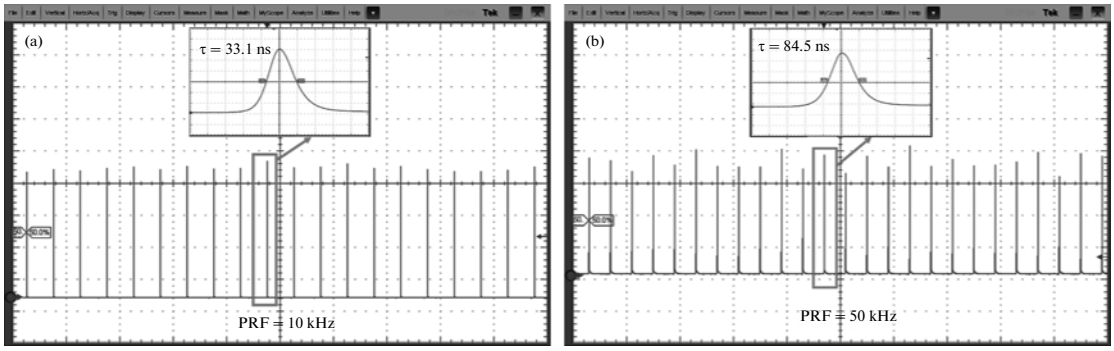

Fig. 7. Pulse trains and typical shapes of the 473 nm blue laser at 10 (a) and 50 kHz (b).

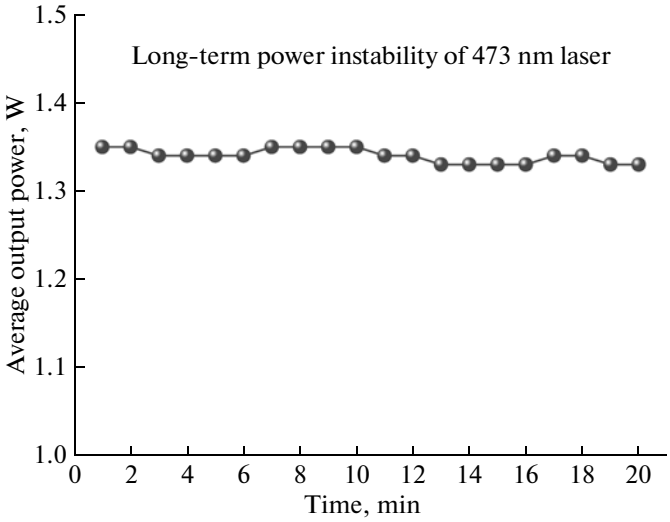

Fig. 8. Long-term power instability test of pulsed 473 nm laser.

perature control in Nd:YAG and BiBO crystals. On the one hand, little temperature fluctuation of the laser medium results in a minor change of the thermal population on the lower level in quasi-three-level laser system, so enhances the output power stability of the fundamental laser. On the other hand, little temperature fluctuation in the nonlinear crystal leads to accurate phase-match between fundamental laser and second harmonic laser.

4. CONCLUSIONS

A high-repetition-rate, high-peak-power Nd:YAG lasers at 946 and 473 nm by intracavity frequency-doubling were demonstrated in this paper. Using a compact V-type laser cavity and a miniature AO Q-switch, an average output power of 4.5 W 946 nm laser was obtained at a repetition rate of 10 kHz. With a BiBO crystal as frequency-doubler, 1.35 W pulsed 473 nm laser was achieved at 10 kHz, with a peak power of 4.1 kW and a pulse width of 33.1 ns. The long-term power stability was less than 1% then. Fur-

thermore, stable pulsed laser operation at 946 and 473 nm can even reach 50 kHz.

ACKNOWLEDGMENTS

We gratefully acknowledge support from the National Natural Science Foundation of China (Grant no. 60978016) and Scientific and Technological Project of Heilongjiang Province (no. GC06A116).

REFERENCES

1. T. Y. Fan and R. L. Byer, IEEE J. Quantum Electron. **23**, 605 (1987).
2. S. Bjurshagen, D. Evekull, and R. Koch, Appl. Phys. B **76**, 135 (2003).
3. C. Czeranowsky, E. Heumann, and G. Huber, Opt. Lett. **28**, 432 (2003).
4. Y. Chen, H. Peng, W. Hou, Q. Peng, A. Geng, L. Guo, D. Cui, Z. Xu, Appl. Phys. B **83**, 241 (2006).
5. Y. F. Lu, X. H. Zhang, J. Xia, G. Y. Jin, J. G. Wang, X. D. Yin, and A. F. Zhang, Laser Phys. Lett. **7**, 335 (2010).
6. J. Tauer, H. Kofler, and E. Wintner, Laser Phys. Lett. **7**, 280 (2010).
7. C. Zhang, X. Y. Zhang, Q. P. Wang, Z. H. Cong, S. Z. Fan, X. H. Chen, Z. J. Liu, and Z. Zhang, Laser Phys. Lett. **6**, 521 (2009).
8. X. Yu, C. Wang, F. Chen, R. P. Yan, X. D. Li, J. B. Peng, and J. H. Yu, Laser Phys. **20**, 1783 (2010).
9. E. J. Hao, T. Li, H. M. Tan, L. Q. Zhang, and Y. Zhang, Laser Phys. **19**, 1953 (2009).
10. Y. F. Lu, X. D. Yin, J. Xia, R. G. Wang, and D. Wang, Laser Phys. Lett. **7**, 25 (2010).
11. C. W. Wang, Y. L. Weng, P. L. Huang, H. Z. Cheng, and S. L. Huang, Appl. Opt. **41**, 1075 (2002).
12. Y. Lutz, D. Rytz, and C. Gaudillat, Appl. Phys. B **70**, 479 (2000).
13. Y. H. Chen, W. Hou, H. B. Peng, H. L. Zhang, L. Guo, H. B. Zhang, D. F. Cui, and Z. Y. Xu, Opt. Commun. **270**, 58 (2007).
14. J. Gao, X. Yu, X. D. Li, F. Chen, Z. Zhang, J. H. Yu, and Y. Z. Wang, Laser Phys. Lett. **5**, 433 (2008).
15. J. Gao, X. Yu, F. Chen, X. D. Li, R. P. Yan, Z. Zhang, J. H. Yu, and Y. Z. Wang, Laser Phys. Lett. **5**, 577 (2008).
16. R. Zhou, E. B. Li, H. F. Li, P. Wang, and J. Q. Yao, Opt. Lett. **31**, 1869 (2006).
17. W. P. Risk, J. Opt. Soc. Am. B **5**, 1412 (1988).
18. J. Gao, J. Speiser, and A. Giesen, in *Advanced Solid-State Photonics*, Technical Digest (Opt. Soc. Amer., 2005), paper TuB34.
19. S. Bjurshagen and R. Koch, Appl. Opt. **43**, 4753 (2004).
20. S. Wang, H. J. Eichler, X. Wang, F. Kallmeyer, J. Ge, T. Riesbeck, and J. Chen, Appl. Phys. B **95**, 721 (2009).
21. T. Baer, J. Opt. Soc. Am. B **3**, 1175 (1986).